Journal of the Korean Society
for Nondestructive Testing
Vol. 28, No. 3 (2008. 6)

Analysis on Thermoelastic Stress in the Cantilever Beam by Lock-in Thermography

K. S. Kang*, M. Y. Choi*, J. H. Park* and W. T. Kim**†

Abstract In this paper, effects of thermoelastic stress by using lock-in thermography was measured in the cantilever beam. In experiment, a circular holed plate was applied to analyze variation of transient stress under the condition of repeated cyclic loading. And the finite element modal analysis as computational work was performed. According to the surface temperature obtained from infrared thermography, the stress of the nearby hole was predicted based on thermoelastic equation. As results, each stress distributions between 2nd and 3rd vibration mode were qualitatively and quantitatively investigated, respectively. Also, dynamic stress concentration factors according to the change of vibration amplitude were estimated for the resonance frequency.

Keywords: Lock-in Thermography, Thermoelastic Stress, Nondestructive Testing, Concentration Factor, Finite Element Modal Analysis

1. Introduction

In structural components subjected to high frequency vibrations, those are usually required to avoid resonance frequencies and broadly used in vibrating parts of gas turbine engines. Although the operating frequency is designed at higher than resonance frequencies, the structure, when a vibrating structure starts or stops, has to pass through a resonance frequency, which results in large stress concentration. The structures, designed in the form of cantilever are widely applied to the wing of aircraft and the turbine blade. The operating frequency of these structures generally are designed at higher than the resonant frequency, to avoid the interference resulted from the resonant frequency. Therefore, these structures must inevitably pass through the resonant frequency band when starting or stopping. It is very important to check the level of stress when these structures operate around the resonant frequency or pass through the resonant frequency before and after the operation(Putter and Manor, 1978). However, most of relevant studies have been focused on the frequency response characteristic of specific structure or motion appeared at the specific resonant frequency. Only a few studies have been conducted on stress distribution appeared on the structure under the transient condition(Yoo et al., 1995). Also, if these structures contain any geometrical discontinuities such as notch and hole, it will cause the instability and destruction of structure by changing the vibration characteristics and stability of structures.

However, it was hard to configure the previous test method, required for measuring the stress on the discontinuous area under the transient condition, with the existing contact type technique, so many researches have predicted the

Received: May 2, 2008, Revised: June 13, 2008, Accepted: June 17, 2008 * Safety Metrology Group, Korea Research Institute of Standard and Science, P.O.Box 102, Yuseong Daejeon, 305-600, Korea, ** Department of Bio-Mechanical Engineering, Kongju National University, Yesan, Chungnam, 340-702, Korea † Corresponding author: E-mail:kwt@kongju.ac.kr

stress distribution through the numerical analysis instead of experimental works (Coda and Venturini, 2000). In this study, it was measured the change of thermoelastic stress distribution by using infrared thermography (IRT), when the cantilever structure with circular hole was operated under the transient condition for the estimation of stress distribution. And then, the dynamic stress concentration factor was predicted nearby hole, which was compared with that of finite element analysis.

2. Thermoelastic Effects

When an object insulated from the external area is deformed or transformed by the external force, thermo-mechanical coupling effect appears. The thermoelastic equation in the elastic interval can be constructd as formula of eqn. (1) (Rauch, and Rowlands, 1993).

$$\rho c \frac{\partial T}{\partial t} = -\frac{E}{1-2\nu} \alpha T_a \frac{\partial \varepsilon}{\partial t} \quad (1)$$

where, ρ, c, T, t, E, ν, α, T_a, and ε indicate the density, specific heat, temperature change of object, time, elastic modulus, poisson ratio, thermal expansion coefficient, ambient temperature and strain, respectively(Panteliou and Dimarogonas, 1997).

The eqn. (1) is expressed in the form of nonlinear equation because of irreversible $\partial\varepsilon/\partial t$ item resulted from the attenuation of material and T_a item being dependent on the time. If the ambient temperature is constant and relation between stress and deformation is maintained as the linear during the test, it may be construed as the linear differential equation and eqn. (1) may be expressed as eqn. (2) (Bremond and Potet, 2001). In this paper, we measure the temperature of subject object using the infrared thermography camera and predict the thermoelastic stress based on the relational expression of eqn. (2). Here, $\triangle\sigma_{1,2,3}$ and K_m indicate the sum of stress measured on 3 axes and thermoelastic coefficient, respectively(Kim et al., 2006; Choi et al., 2008).

$$\Delta T = -\frac{\alpha}{\rho c} T_a \frac{E}{1-2\nu} \Delta\varepsilon = -K_m T_a \Delta\sigma_{1,2,3} \quad (2)$$

3. System Configuration

There is no thermal loss resulted from the conduction and convection. Those must be guaranteed on the specimen and thermal parallel condition guaranteeing no heat exchange must be maintained during the test for the correct analysis of thermoelastic stress. In this study, the thermal parallel condition is guaranteed on the specimen by repeatedly applying the constant frequency and load to satisfy the insulation condition of specimen. Also, since the chamber is applied to maintain the internal temperature, convection, and emissivity, the experiment in the manufactured chamber was considered to be isolated for the heat exchange.

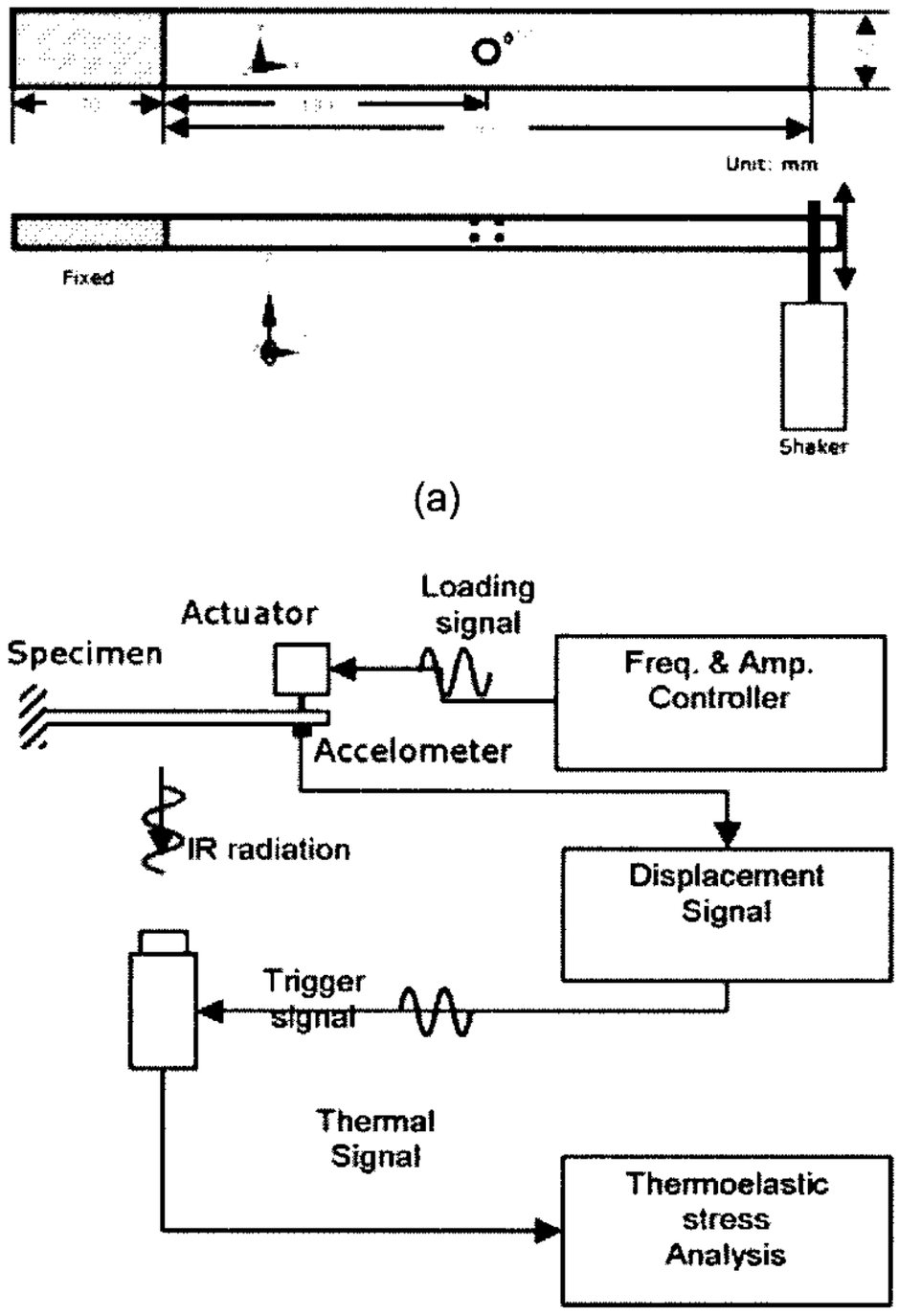

Fig. 1 Schematics diagram for the experiment (a) the shape and boundary condition of the specimen, (b) signal acquisition of measurement system

It is manufactured that the specimen of cantilever type is under the condition of Euler-Bernoulli, so that only the bending load may be applied around the round hole. The material is made of STS304, of which thermoelastic coefficient of 4.51×10^{-12} Pa^{-1}. Fig. 1 shows the shape and boundary condition of specimen and schematic diagram of test system respectively. As experimental measurements, IR camera is used with the model of Sliver 480M manufactured by the Cedip Infrared System. Temperature sensitivity (NEDT) of this detector is within 0.02 ℃. The temperature distributions are measured using the lock-in method, which is synchronizing the infrared detector and specimen[6]. The cantilever beam is vibrated by shaker according to the amplitude and frequency controlled by the function generator and the resonant frequency and amplitude of specimen is analyzed with the accelerometer (352B10, PCB Piezotronics Co.).

The measured resonant frequency is compared with the modal analysis results of finite element analysis and measured acceleration is used to acquire the stress distribution in the finite element analysis. Finally, the stress concentration factor, acquired by the finite element analysis, is compared with stress concentration factor measured by using infrared thermography.

4. Results and Discussions

4.1 FEM Results

Finite element analysis supplies the resonant frequency and vibration mode shape by performing the modal analysis using the commercial program (ANSYS, element shell 181). Then, the stress distribution at each resonant frequency can be acquired by entering the measured acceleration data into FEM analysis.

The Fig. 2 shows the resonant mode and stress distribution at resonant frequency measured using the FEM. From Fig. 2 the resonant mode and stress distribution at each 2nd and 3rd resonant frequency is estimated by FEM. The resonance frequencies are compared with results of accelerometer.

Fig. 2(a) shows the 2nd mode for resonance frequency of 39 Hz by FEM, 35 Hz by accelerometer and Fig. 2(b) shows the 3rd mode at resonance frequency of 109 Hz by FEM, 94 Hz by Accelerometer. From he results of FEM analysis, it shows that the biggest stress is predicted around the round hole in the mode 2. Also, the results show that the nodal line is formed around the round hole in the mode 3 and stress is close to "0" and the biggest stress is measured at the fixed point.

As shown in Fig. 3, it is indicated that the stress distribution in the form of proportion

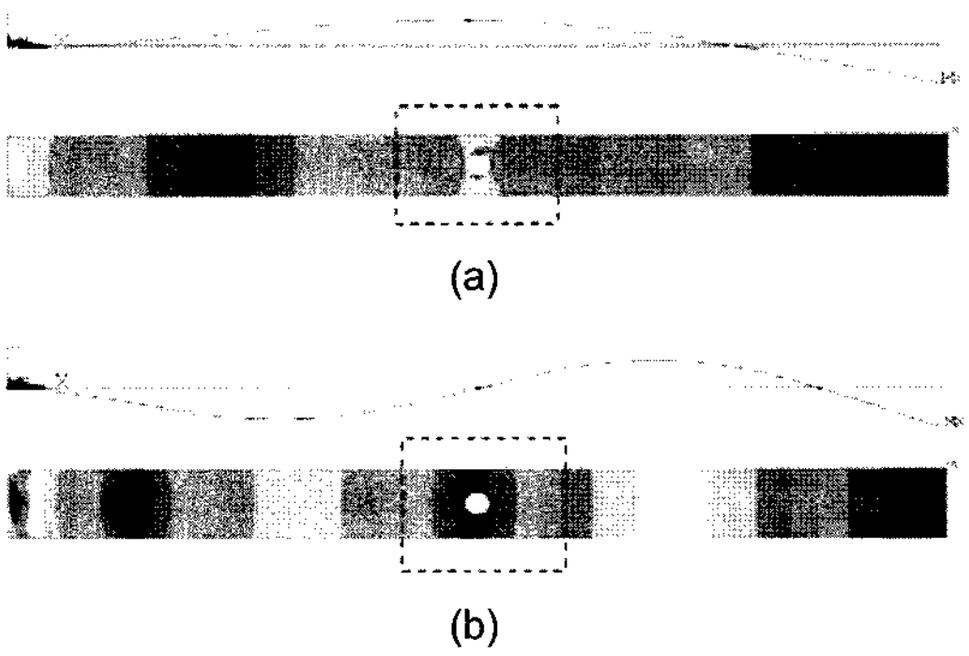

Fig. 2 The resonant mode and stress distribution at each 2nd and 3rd resonant frequency estimated by FEM. (a) resonant mode and stress distribution at 2nd mode, (b) resonant mode and stress distribution at 3rd mode

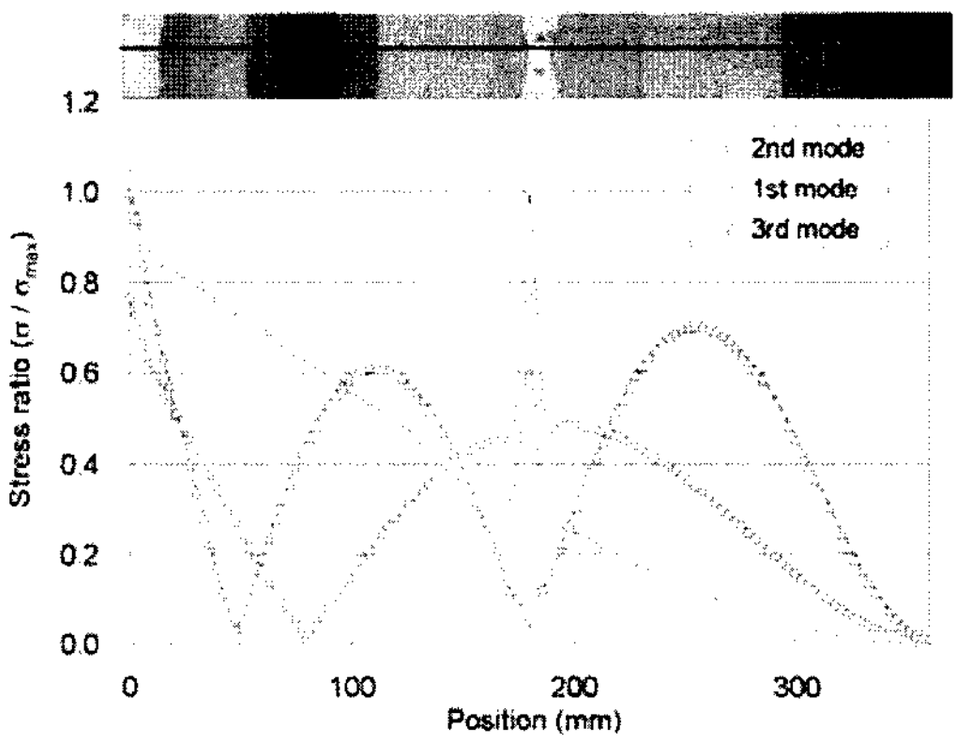

Fig. 3 The change of stress ratio at resonant frequency by FEM

(σ/σ_{max}) based on the maximum stress at each resonant frequency. The analysis results show that the highest stress concentration is measured in the mode 2, so we acquire the stress concentration factor based on the analysis results of mode 2 and then compare the acquired stress concentration factor with the infrared thermography test results.

4.2 Infrared Thermography Results

The infrared thermography test is conducted to analyze the stress distribution resulted from the change of frequency and amplitude. For the frequency change, the stress distribution is measured in the range from 35 Hz to 80 Hz, for resonant frequencies in the mode 2, and 94 Hz, resonant frequency in the mode 3 respectively.

Fig. 4 shows the comparison of stress map at 2nd vibration mode between (a) thermography result and (b) FEM results. As shown in imaging, it shows that the stress distribution is same around the round hole. From the results measured by comparing the stress distribution image acquired using the IRT in the mode 2 with that of FEM analysis. The stress distribution for both shows good agreement.

Fig. 5 shows the change of stress distribution appeared around the round hole according to change of frequency using the infrared thermography. Stress is concentrated around the round hole at frequencies of 35 Hz and 60 Hz.

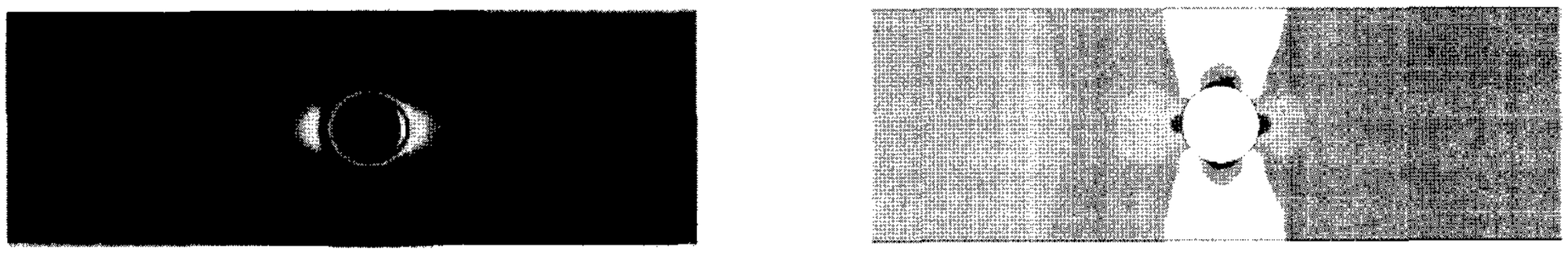

(a) (b)

Fig. 4 Stress map at 2nd vibration mode; (a) thermography imaging, (b) FEM imaging

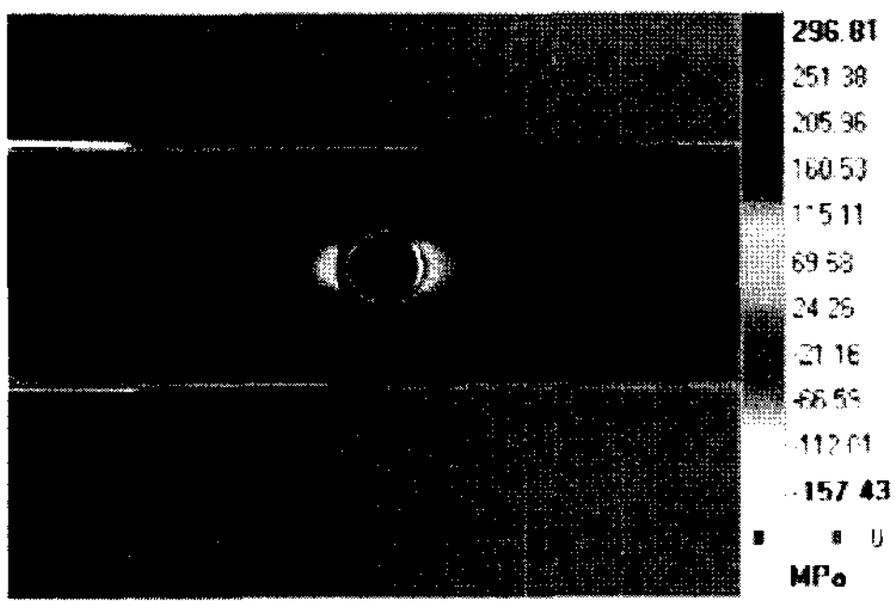

(a) 35 Hz

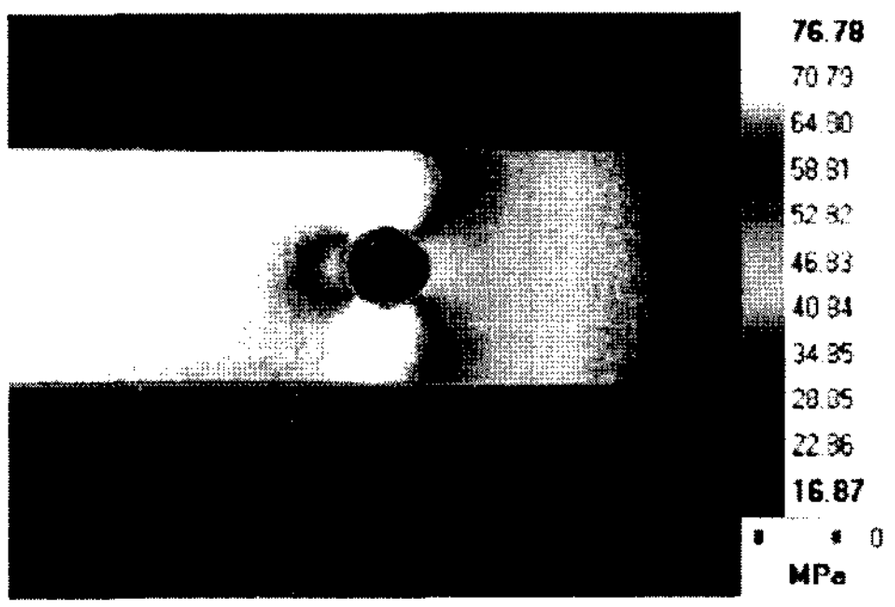

(b) 60 Hz

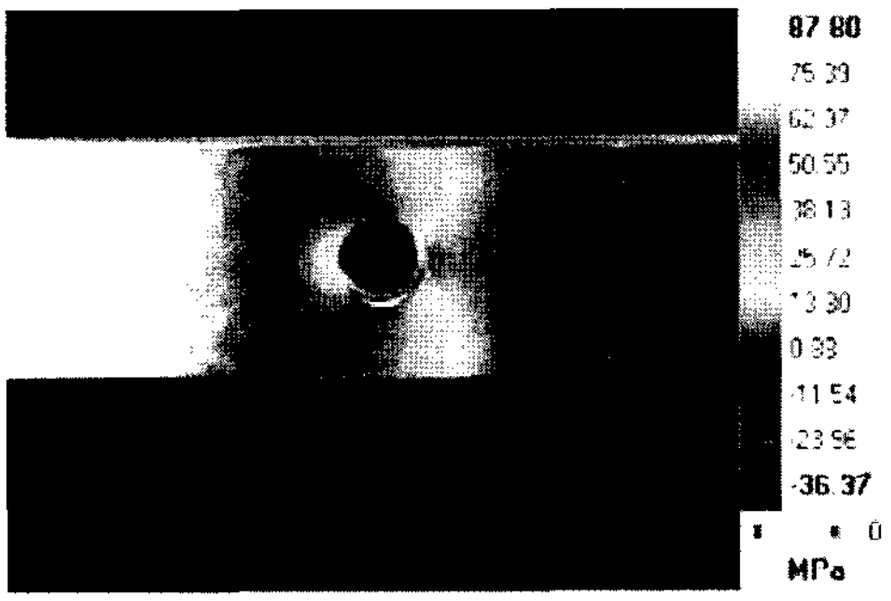

(c) 80 Hz

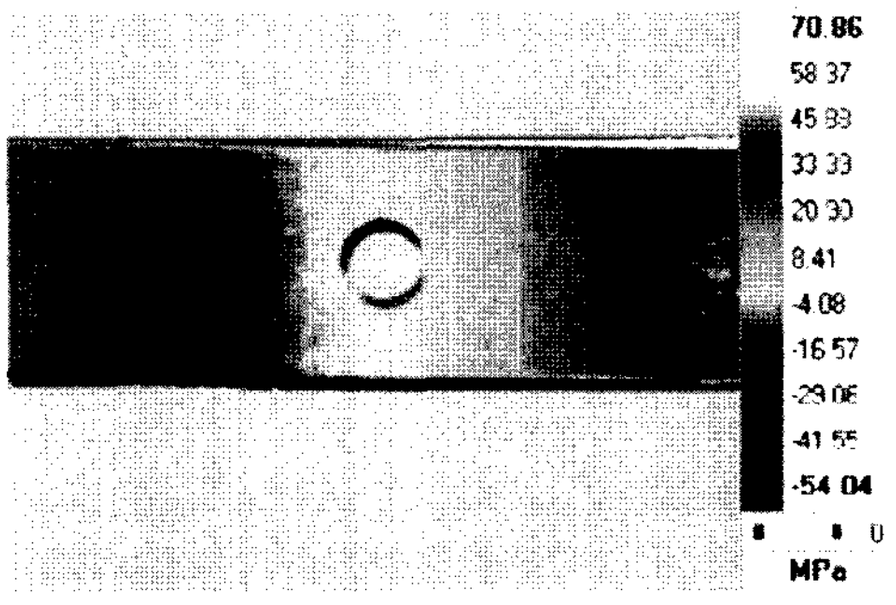

(d) 94 Hz

Fig. 5 Stress distribution around the round hole at the change of frequency in the infrared thermography

Also, these two figures show that the point, where the biggest shearing stress is appeared (stress becomes "0"), moves to the left and is formed at the height of 180 mm in the mode 3 when the frequency is increased. Thus, it might be traced for the change of stress distribution under the transitional condition through the infrared thermography test as shown in Fig. 6. From the figure, the stress distribution proportion (σ/σ_{max}) is appeared around the round hole according to change of frequency.

Fig. 7 shows the dynamic stress concentration factor resulted from the change of shaker amplitude at frequency of 40 Hz, resonant frequency band of mode 2. The excitation amplitude change measured using the acceleration indicates the accelerated value (g, m/s^2). The stress concentration factor is used to

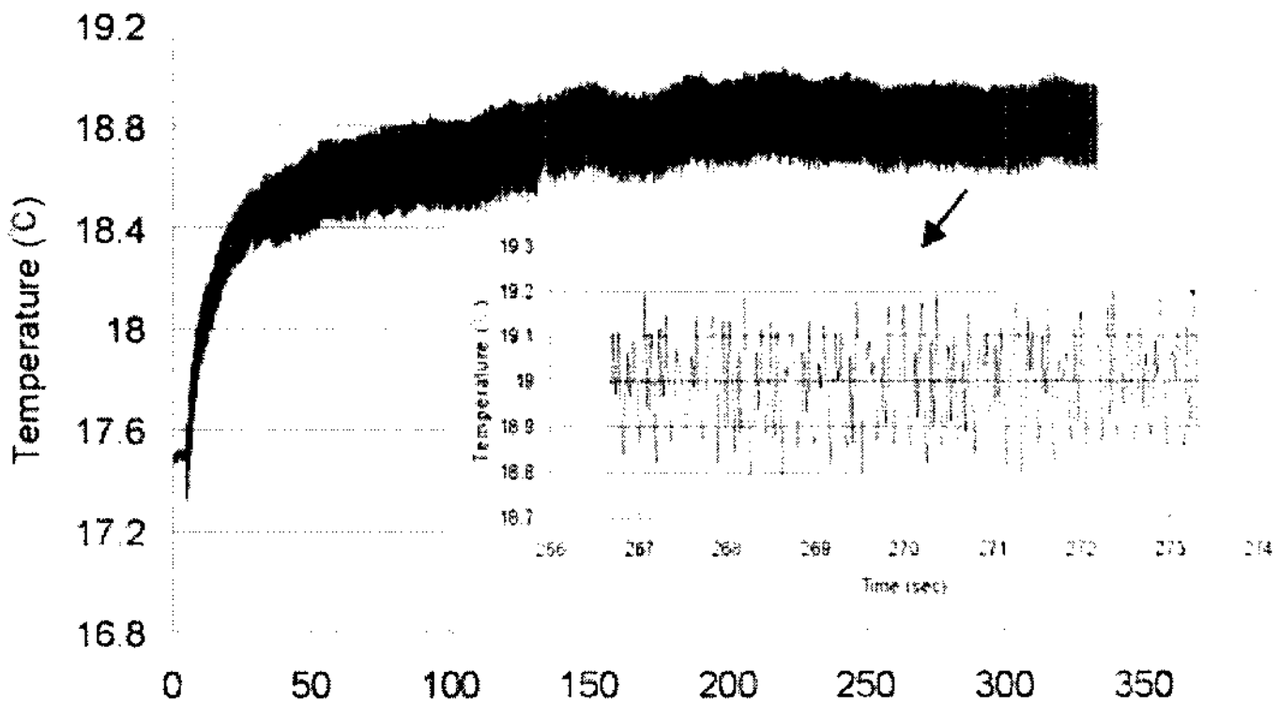

Fig. 6 Temperature rise around the round hole according to change of time

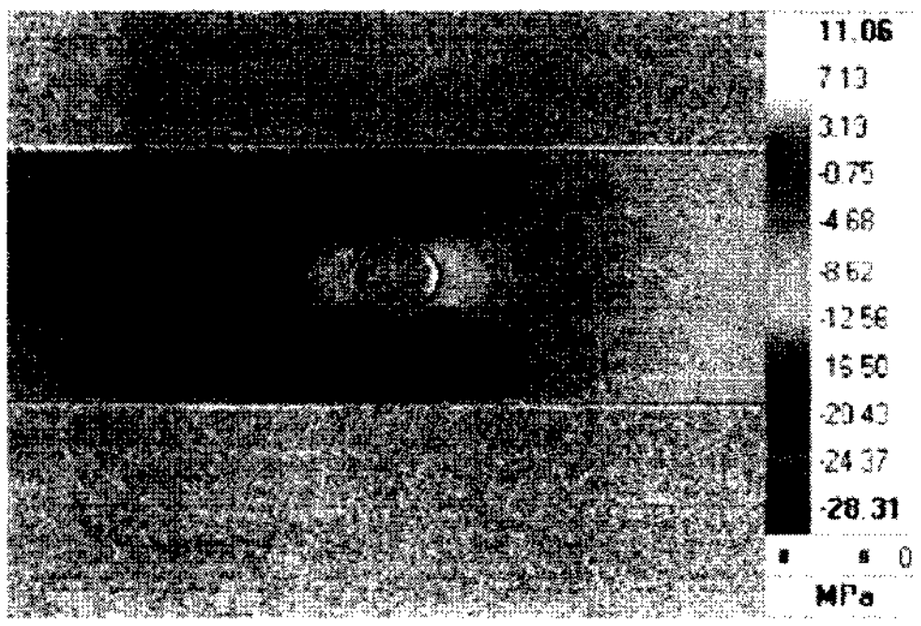

(a) 4 g

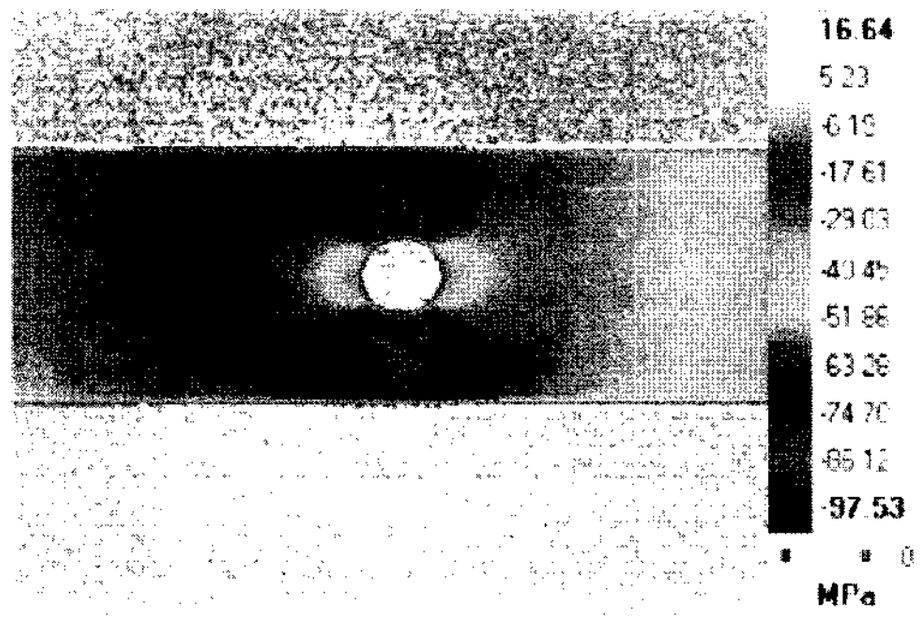

(b) 12 g

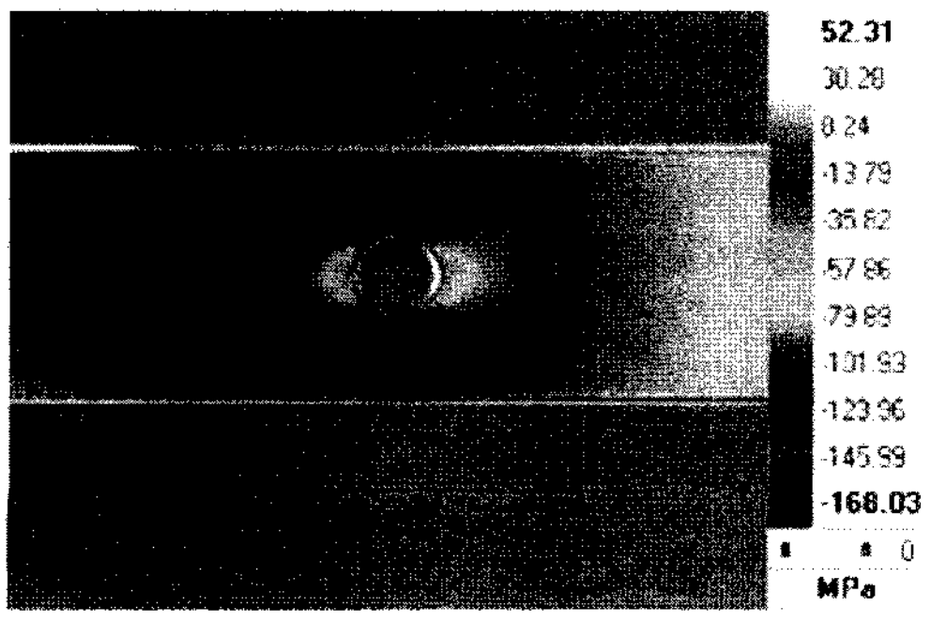

(c) 20 g

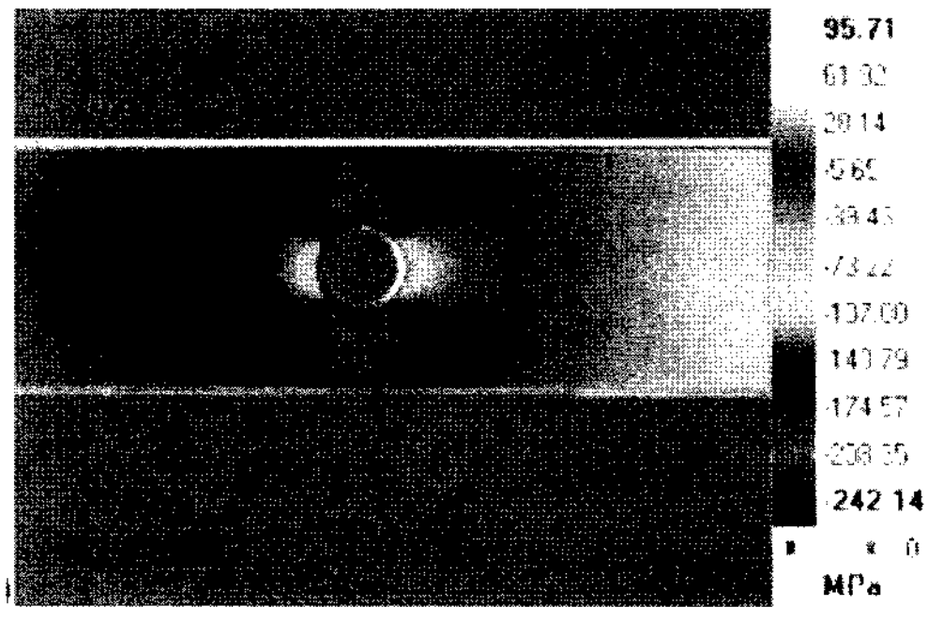

(d) 28 g

Fig. 7 Dynamic stress concentration factor for each change of shaker amplitude at frequency

acquire the average stress (σ_{Avg}) in the areas of 195 ~ 210 mm and express the stress ratio (σ/σ_{Avg}) for each location. The stress concentration factor acquired using the FEM is evaluated as 2.07 and measured as 1.75 ~ 1.92 in the infrared thermography test. The average of test results is evaluated as 1.85. The error between infrared thermography test and FEM is evaluated as 10.6 %, so the error rate is evaluated to be relatively correct.

5. Conclusions

In this paper, we measure the stress distribution of structure designed in the form of cantilever under the transient condition using the infrared thermography and predict the dynamic stress concentration factor based on the stress distribution. Test results shows the change of stress distribution resulted from the frequency change measured in the resonant modes 2 and 3. Stress concentration factor resulted from the change of amplitude at frequency of 40 Hz is estimated and then the value is compared with results of finite element analysis. The relative measuring error is measured as 10.6 % because the spatial resolution of detection device is so limited and experimental system does not completely meet the thermal parallel condition of specimen. The many advantages of infrared thermography such as non contact, whole field, insensitivity of environmental vibration enables its user to measure the stress of small and micro structure, without shape limitation.

Remarks

This work was supported by the Korea Science and Engineering Foundation (KOSEF) grant funded by the Korea government(MOST) (No.2008-00467)

References

Bremond, P. and Potet, P. (2001) Lock-In Thermography: A Tool to Analyze and Locate Thermo-Mechanical Mechanisms in Materials and Structures, Thermosense XXII, pp. 4360-4376

Choi, M., Kang, K., Park, J., Kim, W. and Kim, K. (2008) Determination of Size and Location of a Subsurface Defect of Reference Specimen, Journal of NDT & E Int., Vol. 41, No. 2, pp. 119-124

Coda, H. B. and Venturini, W. S. (2000) *Dynamic Non-Linear Stress Analysis by the Mass Matrix BEM - Eng. Analysis with Boundary Element*, Vol. 24, pp. 623-632

Kim, W., Choi, M. and Park, J. (2006) NDT Analysis of Metal Materials with Internal Defects Using Active Infrared Thermography Method, Journal of Key Engineering Materials, Vols. 321-323, pp. 835-840

Panteliou, S. D. and Dimarogonas, A. D. (1997) Thermodynamic Damping in Porous Materials with Ellipsoidal Cavities, Journal of Sound and Vibration, Vol. 201, No. 5, pp. 555-565

Putter, S and Manor, H. (1978) Natural Frequencies of Radial Rotating Beams, Journal of Sound and Vibration, Vol. 56, pp. 175-185

Rauch, B. J. and Rowlands, R. E. (1993) *Thermoelastic Stress Analysis in Handbook on Experimental Mechanics*, Edited by Kobayashi, A. S., SEM, pp. 280-295

Yoo, H., Ryan, R. and Scott, R. (1995) Dynamics of Flexible Beams Under Overall Motions, Journal of Sound and Vibration Vol. 181, No. pp. 261-278